A theoretical study of selenium I under high pressure

1993 J. Phys.: Condens. Matter 5 8065

(http://iopscience.iop.org/0953-8984/5/43/018)

J. Phys.: Condens. Matter 5 (1993) 8065–8074. Printed in the UK

A theoretical study of selenium I under high pressure

Hadi Akbarzadeh†, Stewart J Clark and Graeme J Ackland
Department of Physics, The University of Edinburgh, Edinburgh EH9 3JZ, UK

Received 9 July 1993

Abstract. Using recently developed codes for density-functional total-energy calculations we trace the structural and electronic response of the hexagonal phase of selenium to applied pressure. We find that the anomalous linear expansion coefficient is well reproduced, and the structure reduces its volume by straightening its twofold-coordinated chains and bringing them closer together. The characteristic overbinding of the local-density approximation causes an effect akin to a spurious pressure on the system rather than a straightforward volume rescaling. The model also predicts a band gap closing rapidly with pressure within the same structural space group. This is not the observed metallization pressure, which in practice is induced by a structural phase transition. We further show that the valence bands are correctly associated with covalent bonds, lone pairs and s-type atomic orbitals, with the lone pairs being the least strongly bound.

1. Introduction

The behaviour of selenium under pressure has attracted a great deal of interest for many years. The ambient pressure phase has hexagonal symmetry with space group $P3_121$ D_3^6. This consists of twofold-coordinated helical chains of atoms running along the c direction and close packed in the plane perpendicular to it (figure 1). The structure has a highly anisotropic response to increasing pressure: the material expands along the c axis while contracting along a [1]. The opposite behaviour is observed with temperature, the c axis showing negative linear thermal expansion while large positive expansion along a leads to overall volume expansion. In addition to this anisotropy, the elastic constants themselves have a large non-linear dependence on the pressure.

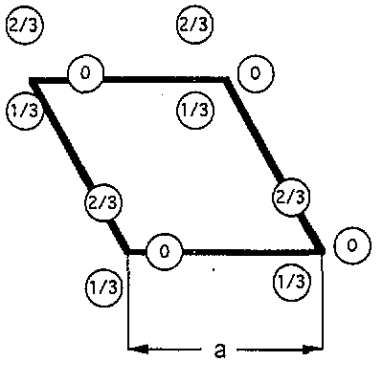

Figure 1. Projection diagram of the selenium I structure along the c axis.

† On sabbatical leave from Isfahan University of Technology, Isfahan, Iran.

0953-8984/93/438065+10$07.50

This behaviour can be explained by a simple empirical argument comparing the relative strengths of the intrachain (covalent) bonds and the interchain bonds [2]. With increasing pressure the chains approach each other more closely and the interchain bonds become stronger. In the extreme case it is mathematically possible to make the interchain and intrachain bonds the same length, in which case the structure becomes sixfold coordinated although its space group is unchanged. This gives a plausible route through a continuous metallization transition. In practice, however, increasing pressure results in a first-order phase transition before the equalization of bondlengths can occur.

In addition to the hexagonal form, there are numerous metastable forms of selenium, including an amorphous form consisting of intertwined chains. The bonding in these chains is similar to that observed in the hexagonal phase. Modelling the behaviour of such amorphous material is currently beyond the scope of *ab initio* calculation because of the lack of periodicity and the importance of entropic effects. It is possible, however, to use empirical force-field models, an essential ingredient of which is the relative strengths of the inter- and intrachain bonds, both in formation and distortion. Accurate determination of these forces at a range of separations, as presented here, should facilitate such potential development.

The nature of the pressure-induced transition and the first high-pressure phase, selenium II, is still controversial [3,4]. Some groups have reported a second semiconducting phase prior to the metallization transition [5]. No structural solution of this phase has been presented, but a layered structure seems most likely. Other studies have not observed this intermediate phase [4], reporting the first structural phase transition as going directly to a metallic phase.

2. Calculational details

The calculations were performed using the CASTEP code, which has been documented in detail elsewhere [6,7]. This code solves the Kohn–Sham equations [8] with the exchange and correlation energies [9] being treated within the local-density approximation (LDA). The wavefunctions are expanded in a plane-wave basis set with periodic boundary conditions. In the present case this type of basis set is ideal to avoid biassing the calculation toward bonding or dangling orbitals, and also because the basis set remains unaltered if the atoms are moved, so no Pulay [10] forces arise and it is possible to relax the atomic positions using forces calculated from the Hellmann–Feynman theorem. The self-consistent electronic relaxation is carried out using a conjugate-gradients method with corrections to maintain orthonormality. The first three complete shells are treated using a norm-conserving, non-local pseudopotential of the Kleinmann–Bylander [11] type, generated by Lin and co-workers [12] using the method of Kerker [13]. The plane-wave basis set is cut off at 300 eV, further increase did not change the results significantly.

Although relaxation of the atoms was done directly, using the Hellmann–Feynman forces and a steepest-descents algorithm, relaxation of the unit cell was achieved by performing a series of runs at various c and a parameters, in each case relaxing the atomic positions. The energy changes much faster with volume than c/a, so we made our initial guesses by assuming volumes near to the experimental one, and using several c/a ratios to locate the energy minimum (i.e. the hydrostatic configuration corresponding to that volume). We used all our runs to produce contour plots of enthalpy against c and a for various pressures—the minimum of such a plot corresponds to the hydrostatic configuration at that pressure; all calculations are effectively at 0 K so entropic effects can be ignored. We present an example

of these data in figures 2 and 3 which shows the enthalpy against volume and c/a at zero pressure.

The problem of k-point sampling is particularly acute in the present case. With a high degree of symmetry, to calculate the energy it is sufficient to calculate the wavefunctions based on several k points in the irreducible slice of the Brillouin zone only. The energy at equivalent points is identical. If the cell is not centrosymmetric, this may not be true for the Hellmann–Feynman forces however. With few k points, we found that the sampling was too poor to give forces independent of choice of k point, and relaxation to the apparent minimum energy structure broke hexagonal symmetry. With many k points, rounding errors in the forces tended to destabilize the relaxation and make the calculations very slow. The solution to this is to take advantage of the symmetry of the structure.

There are a number of parts of the calculation which should reflect the full symmetry of the lattice. In particular, the charge density and the atomic forces should all be symmetric. We enforce this by averaging the charge density from each k point at each equivalent point in the Brillouin zone, to obtain an averaged reciprocal charge density in the irreducible slice of the zone and identical charge densities in equivalent regions. The symmetric charge density in real space is then obtained by a Fourier transformation of this reciprocal quantity. This procedure ensures that the charge density has the correct symmetry for the hexagonal selenium structure.

The Hellmann–Feynman forces calculated with this charge density now reflect the symmetry of the lattice, but the non-local contribution to the forces still does not [7]. Therefore prior to relaxing the ions under the forces (averaged over k points) it is necessary to symmetrize the forces still further, so that the $P3_121$ D_3^6 symmetry is not broken.

A disadvantage with this method is that the energy functional is no longer exactly variational with respect to the atomic positions, although it is nearly so and in the limit of many k points (or a set of k-point stars containing the full lattice symmetry) it will become so. Consequently, when relaxing the ions under the symmetrized forces we use a steepest-descents algorithm that does not use information about the total energy.

This procedure allows us to use only special k points, and we used the sets of special k points suggested by Chadi and Cohen [14] for the hexagonal lattice. Comparing results for a few c/a ratios obtained with trial sets of 4, 6, 10 and 12 k points, we found no significant difference between 10 and 12 and so have carried out the calculations with 10 special k points, which correspond to 27 k points in the whole Brillouin zone. Subsequent calculations using very many k points to determine band structures further suggest that the 10 k-point set is sufficient for relaxation purposes.

We find that the energy converges to about 0.01 eV per atom while the forces are of the order of 0.05 eV $Å^{-1}$.

3. Structural dependence on pressure

The calculated minimum-energy structure has lattice parameters $a = 4.12$ Å, and $c = 5.06$ Å (figure 2) as compared to the experimentally observed $a = 4.37$ Å, $c = 4.96$ Å [3,4]. As is usual with LDA calculations, the calculated volume is about 9% smaller than the experimentally observed 81.9 $Å^3$ per unit cell (about 1% of this can be accounted for by thermal expansion since the experiments were carried out at room temperature). However, the theoretical c parameter is actually larger than the experimental value: we shall return to this point later.

As a result of symmetry constraints, the internal structure can be described by a single parameter and the unit cell by the volume and c/a ratio. The evolution of these with

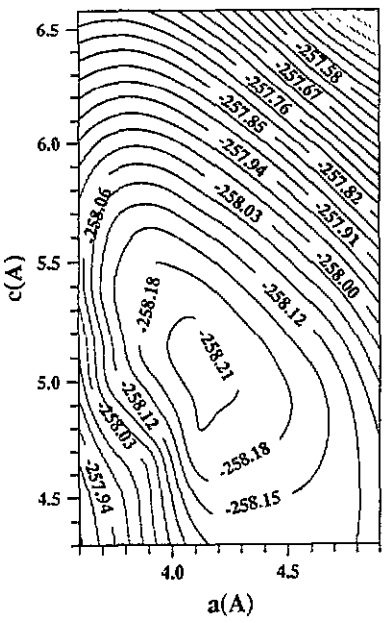

Figure 2. Total energy (in eV per atom) surface of the internally relaxed structure plotted against c and a parameters for hexagonal selenium.

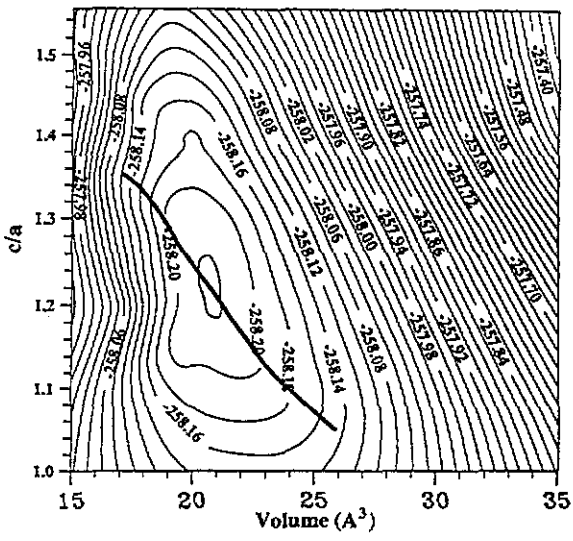

Figure 3. Total energy (in eV per atom) surface of internally relaxed structures plotted against c/a ratio and volume per atom. The thick curve passes through those configurations corresponding to hydrostatic pressure.

increasing pressure is shown in figures 3 and 4. The rapid increase of c/a with increased pressure (reduced volume) results from the chains being pushed closer together (it is much easier to compress the interchain bonds than the intrachain covalent bonds). The increase in u is in part commensurate with the reduction in a while maintaining the chains relatively intact. The solid curve in figure 4 shows how u would vary directly as a result of reduced a if the chains remained unaffected, simply moving closer together (i.e. with constant c, bond length and bond angle). The excellent fit of this curve to the data suggests that this simple model of compression in selenium is appropriate.

To compare meaningfully with experiments at high pressure it is necessary to consider c/a values along the hydrostatic curve in figure 3. Other configurations are of little practical interest: they correspond to non-hydrostatic elastic strains, and in practice such strains of any significant magnitude will lead to plastic deformation. After a spread of calculations across a–c space, we were able to deduce the approximate position of the hydrostatic curve and concentrate further calculations along it.

The gradient of the hydrostatic curve alone can be used to deduce the ratio of the linear expansion coefficients. The exact values can be determined from the bulk modulus as described below. We find that $(\mathrm{d}c/c\,\mathrm{d}P)/(\mathrm{d}a/a\,\mathrm{d}P) = -0.45$, in excellent agreement with the experimental value [15]. The negative sign arises because c actually increases with applied pressure (isotropic compression would lead to a ratio of unity).

Figure 5 shows a plot of energy against volume along the hydrostatic curve. This figure can be deduced from the hydrostatic curve in figure 3. We fitted it to a Murnaghan [16] equation of state from which we extract a bulk modulus of 39.5 GPa; this is significantly higher than the experimental value of 14.9 GPa [15], but figure 4 shows that the fit is very poor. We deduce that selenium does not obey a Murnaghan equation of state. This is because

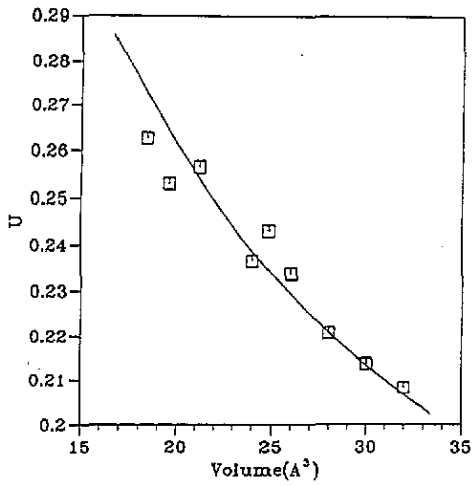

Figure 4. Variation of the internal structural parameter u with atomic volume; these values are taken from points close to the hydrostatic line, and the apparent scatter is due largely to non-hydrostatic effects. The solid curve shows the evolution of u in the simple model that the chains are unaffected and pressure merely reduces their separation. To plot this line we chose values of bond length r = 2.37 Å and bond angle $\theta = 104^{\circ}$.

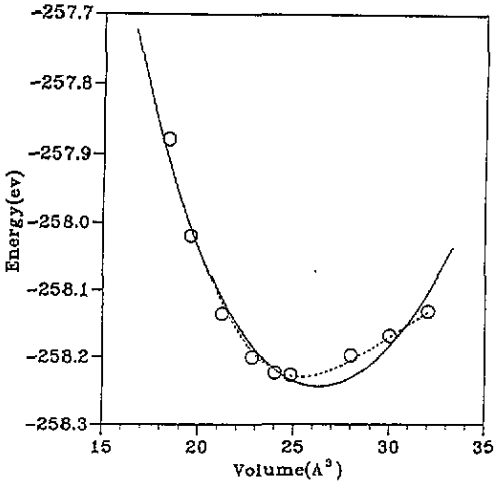

Figure 5. Graph of total energy against volume per atom for structures along the hydrostatic curve for hexagonal selenium. The solid curve shows the best fit to a Murnaghan equation of states, while the dotted curve is a fifth-order polynomial fit.

the Murnaghan equation assumes a linear variation of bulk modulus with pressure, and in this case where the resistance to compression arises initially from weak interchain bonds then increasingly from stronger intrachain bonds, we would not expect a linear variation. Consequently we used a fifth-order polynomial fit to obtain a more reliable estimate of the curvature. This suggests a bulk modulus of 16.8 GPa.

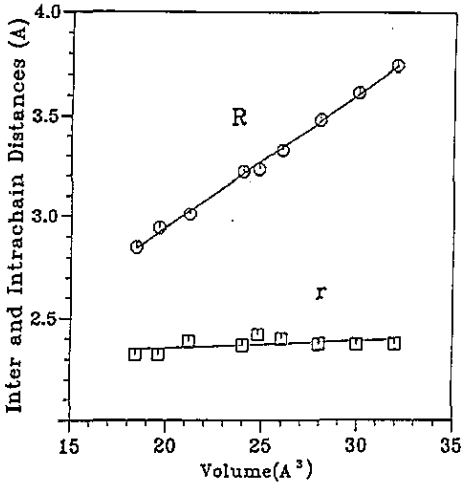

Figure 6. Hydrostatic variation of interchain (R) and intrachain (r) distances with atomic volume; circles and squares are points calculated by interpolation to the hydrostatic curve of a series of constant-volume runs with different c/a.

The mechanism of compression by pushing the chains closer together is illustrated in figure 6 which shows the variation of the interchain (R) and intrachain (r) distances with

cell volume along the hydrostatic line. These are related to the u, c and a parameters by the relations

$$r = \sqrt{3u^2a^2 + (1/9)c^2} \tag{1}$$

$$R = \sqrt{a^2(1 - 3u) + r^2}. \tag{2}$$

The variation of r and R with volume is in extremely good agreement with the experimentally observed data [15].

One curious feature already alluded to is that although the hydrostatic line passes very close to the experimentally observed equilibrium c and a parameters, it does so at a small effective negative pressure. The propensity of LDA to overbind is well known, as is its tendency to predict lattice parameters slightly too low [6]. As far as we are aware this is the first fully relaxed calculation in a material with a negative linear thermal expansion, and as such the first in which it is possible to distinguish between systematic errors in volume and in pressure. Our calculations strongly underestimate the a parameter, but *overestimate* c, at variance with the expected LDA discrepancy in lattice parameter.

A plausible explanation for this is that the overbinding due to the LDA induces a spurious extra pressure on the system. We are unaware of previous work on systems in which this would have been indistinguishable from an underestimate in the length parameters, but here the two can be distinguished because c is known to increase with pressure.

4. Band structure

Once the relaxed atomic structure has been calculated at a given pressure, it is possible to calculate the band structure. The variational density-functional approach does not require exact evaluation of the eigenfunctions of the Kohn–Sham Hamiltonian, since any linear combination will give the same charge density and hence the same physics within the density-functional formalism. To evaluate the band structure requires full diagonalization of the Hamiltonian matrix—a considerably more computation-intensive task. For this reason, we evaluate the charge density using the standard iterative method, then diagonalize the Hamiltonian once only, without any further self-consistency loops. For band-structure calculation it is necessary to evaluate eigenfunctions at many k points; we perform the diagonalization at each of these many k points for the Hamiltonian based on the symmetrized 10-special-k-point charge density.

In figure 7 we show LDA band structures calculated at three different unit cells on the hydrostatic curve. From the tangent to the curve of figure 5 we can estimate the pressure to which these cells correspond. The band structure is in good agreement with previous empirical pseudopotential work [17], which used empirical data to determine the atomic positions. Our calculation is fully *ab initio* both in pseudopotential generation and determination of atomic positions. It shows three low-lying bands and six higher occupied bands. By enforcing symmetry we are also able to study the band structure at pressures beyond that where the real material has undergone a phase transition.

At zero pressure the band gap is 0.5 eV, a direct gap at the H point. At higher pressures this band closes progressively until by 20 GPa it goes to zero and the material undergoes a semiconductor–metal transition. The band closure occurs at the H point. This is the highest pressure at which we performed structural relaxation, and similar to the experimentally observed metallization pressure, derived from resistivity measurements [20], which may be accompanied by a structural phase transition [3,4]. Because of our symmetrization

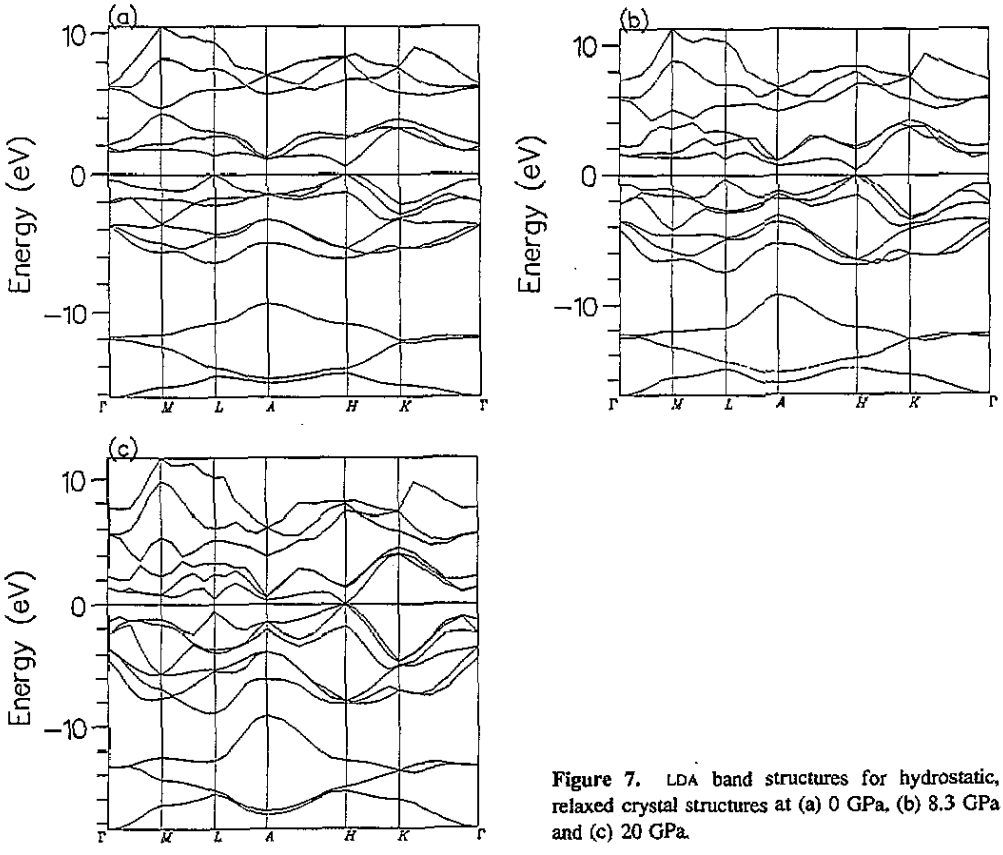

Figure 7. LDA band structures for hydrostatic, relaxed crystal structures at (a) 0 GPa, (b) 8.3 GPa and (c) 20 GPa.

procedure this experimentally observed first-order metallization transition is not permitted by the relaxation procedure.

It should be mentioned that there are several sources of error in calculation of this bandgap and metallization pressure. In the first case, it might be correct to add the 'apparent' pressure arising from LDA overbinding. In addition, it is well established that the one-electron wavefunctions used in the density functional approach do not correctly describe the many-body nature of the exchange and correlation energies [18, 19]. This error is particularly severe for excited states, and leads to an underestimate of the initial band gap.

We have also calculated the band gap at the experimentally observed values of u, c and a where we find it to be 1.13 eV. The 'fictitious pressure' arising from the LDA is about 1.5 GPa, so the band gap opens very rapidly as the chains are pulled apart. A similar dependence of gap on chain separation has been observed in a series of experiments on the $Se_{1-x}Te_x$ system [21], where the chain separation is controlled by concentration.

It is also interesting to note that the closure of the valence–conduction band gap occurs at roughly the same pressure as that at which the gap between the three low-lying states and the six higher valence states closes.

5. Nature of bonding

The band structure shows a clear division between the three lowest-lying bands and the six higher bands. The lower bands have been variously interpreted as s bands, by analogy with

the free-atom data, and as two-centre σ bonding orbitals. The plane-wave basis set used in the current method has no inherent bias toward atomic or bonding orbitals, so it is interesting to examine which picture is more appropriate. Figure 8(a) shows the electron probability density arising from the three lowest-lying Kohn–Sham eigenfunctions only (as determined during the band-structure calculation by matrix diagonalization) in a plane perpendicular to the c direction containing an atom. It is clear that this is predominately spherical and centred on the atom. Consequently, the s-band interpretation of these orbitals is the most appropriate.

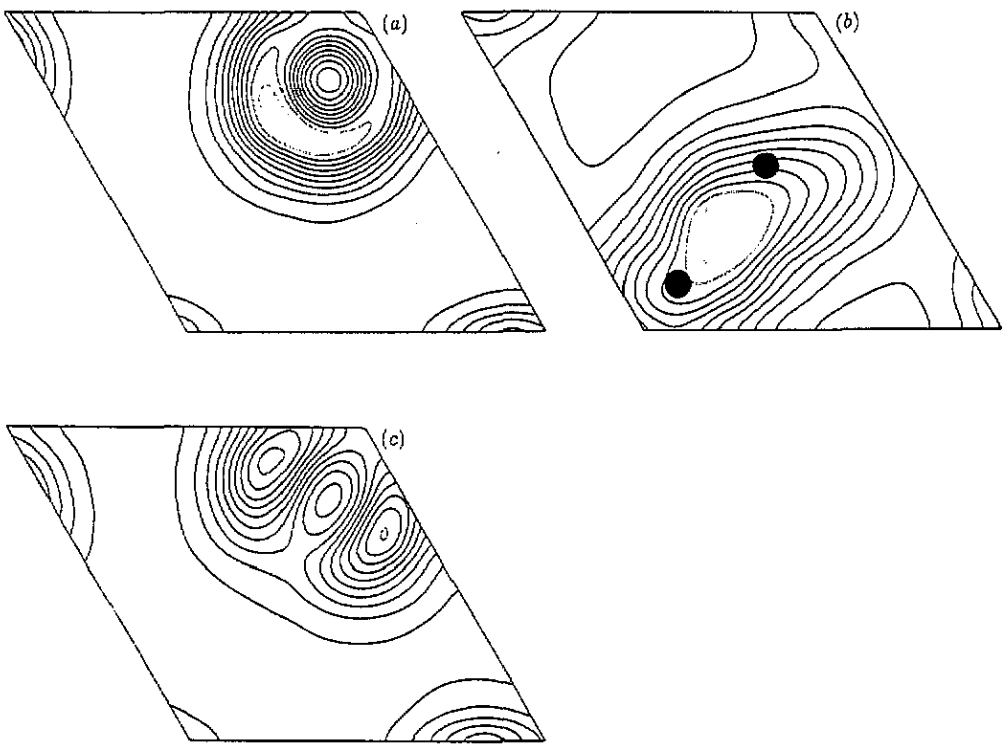

Figure 8. Plot of total electron probability density in the equilibrium structure for eigenfunctions of the three (a) lowest-lying bands (s orbitals), (b) central bands (covalent bonds) and (c) upper bands (lone pairs). The black circles show the location of the atoms; in (b) these have been projected onto the intermediate plane.

The equivalent plot for the sum of the six highest bands (not shown) reveals a similar picture of approximately spherical charge density around each atom. To probe more deeply we divided the bands again into two further groups of three (a reasonably clear separation is indicated by the band structure) and examined planes other than those containing the atom. Now the difference becomes more evident: the central three bands represent covalent bonds and the three uppermost bands represent the lone pairs.

These p-bands are illustrated by figure 8(b), which shows the electron density due to the central three bands on a plane midway between two atoms, with a maximum in the charge density midway between the atoms. A plot of the central three bands in the plane of the atom (not shown) reveals a significant amount of charge in a 'back bond' lying in

the plane: this is consistent with the interpretation of a predominantly p-type character to the bonds. Figure 8(*c*) represents the upper three bands in the same plane as figure 8(*a*). The majority of the charge here is concentrated in lobes directed away from the chain, and the obvious interpretation to place on these is that they represent lone pairs.

6. Discussion

We have calculated the response to pressure of the hexagonal phase in selenium using a total-energy pseudopotential method in the LDA. This model accurately describes the evolution of the internal structure and unit-cell dimensions with pressure. The picture of selenium as a close packed array of infinite spiral chains with only weak interchain bonding is clearly confirmed. There are three possible responses to pressure by which a spiral chain structure can reduce its volume: bringing the chains together, straightening the chains to enable closer packing and reducing the bond length within the chains. At low pressures the first two of these occur, resulting in increased c parameter as the spiral is stretched out with very little reduction in bond length. As the chains approach the overlap between their charge densities increases and the band gap begins to close. In principle this could continue and would be a mechanism for metallization, but in practice a structural phase transition occurs prior to this. The nature of this next high-pressure phase is contentious, but one candidate resembles a chain structure wherein the threefold helical spiral is flattened into a twofold zig-zag, and as the chains are forced closer together cross bonds form creating a fourfold-coordinated corrugated plane [3].

The dispersion of the valence band structure is well reproduced, although the ambient pressure gap of 0.5 eV compared to the 1.8 eV observed experimentally [21] has an error typical of the incorrect treatment of the many-body nature of excited states within the density-functional theory. If the band gap is calculated with the experimentally observed unit cell, a value much closer to experiment is obtained, although recent analysis suggests this is merely due to a cancellation of errors [22]. This gap closes quickly with pressure, until the calculation predicts a metallization transition at 20 GPa. The metallization transition has actually been reported at 23 GPa [20] to be accompanied by a structural transition [3, 4].

We found that a pressure-induced metallization within this space group would theoretically occur at a pressure well before the interchain bond lengths become similar to the intrachain bonds, and hence with a structure which could still accurately be described as consisting of linear chains of covalently bonded twofold-coordinated atoms. We note, however, that in practice selenium exposed to high pressures undergoes a first-order transition to a structure with a different space group at the same time as it metallizes.

The charge densities associated with each band enable us to relate the density-functional approach to the chemical picture of covalency and lone pairs. The three lowest-lying valence bands have atom-centred s-like nature, the middle three represent covalent bonds with charge piled up between the atoms, and the upper three correspond to lone pairs with lobes of charge pointing away from the chain. At higher pressure the s and p bands begin to overlap and eventually this hybridization leads to fourfold-coordinated metallic planar structures. Coincidentally, the band gap between occupied and unoccupied states also closes as the s and p levels overlap.

The usual errors associated with LDA—overbinding and underestimation of the volume—were observed. The anomalous linear expansivities enable us to show that the error in lattice parameter is more akin to an external pressure than to a rescaling of length. Likewise the significant error in the LDA bandgap suggests that the actual pressure calculated for

metallization may be unreliable, although explanations for the band-gap discrepancy suggest that it should vanish as the band gap goes to zero, in which case the calculated pressure would be accurate.

Acknowledgments

We would like to thank H Kawamura and Y Akahama for bringing this fascinating problem to our attention. We would especially like to thank P D Hatton and J Crain for many useful discussions regarding the experimentally known structures in selenium. We thank other members of the 'UK Condensed Matter Grand Challenge', especially V Milman and M C Payne for a copy of their CASTEP code, and V Heine and M J Gillan for sharing their experience and offering advice with the k-point sampling problem. HA thanks Isfahan University of technology and G S Pawley for support during a sabbatical, GJA would like to thank BP and the Royal Society of Edinburgh for supporting a fellowship and SJC thanks the SERC for support. We have also received considerable assistance in the form of computing time from the Edinburgh Parallel Computing Centre and DEC during the testing of their Alpha chip.

References

[1] McCann D R, Cartz L, Schmunk R E and Harker Y D 1972 *J. Appl. Phys.* **43** 1432
[2] Martin R M, Fjeldly T A and Richter W 1976 *Solid State Commun.* **18** 865
[3] Akahama Y, Kobayashi M and Kawamura H 1993 *Phys. Rev.* B **47** 20
[4] Parthasarathy G and Holzapfel W B 1988 *Phys. Rev.* B **38** 10 105
[5] Mao H K, Zou G and Bell P M 1980 *Carnegie Inst. Washington Yearbook* **80** 293
[6] Payne M C, Teter M P, Allan D C, Arias T A and Joannopolous J D 1992 *Rev. Mod. Phys.* **64** 1045
[7] Teter M P, Payne M C and Allan D C 1989 *Phys. Rev.* B **40** 12 255
[8] Kohn W and Sham L J 1965 *Phys. Rev.* **140** 1133A
[9] Perdew J P and Zunger A 1981 *Phys. Rev.* B **23** 5048
[10] Pulay P 1069 *Mol. Phys.* **17** 197
[11] Kleinmann L and Bylander D M 1982 *Phys. Rev. Lett.* **48** 1425
[12] Lin J S, Qteish A, Payne M C and Heine V 1993 *Phys. Rev.* B **47** 4174
[13] Kerker G P 1980 *J. Phys. C: Solid State Phys.* **13** L189
[14] Chadi D J and Cohen M L 1973 *Phys. Rev.* B **8** 5747
[15] Keller R, Holzapfel W B and Schulz H 1977 *Phys. Rev.* B **16** 4404
[16] Murnaghan F D 1944 *Proc. Natl. Acad. Sci. USA* **30** 244
[17] Wendel H, Martin R M and Chadi D J 1977 *Phys. Rev. Lett.* **38** 656
[18] Perdew J P and Levy M 1983 *Phys. Rev. Lett.* **51** 1884
[19] Sham L J and Schluter M 1985 *Phys. Rev.* B **32** 3883
[20] Bundy F P and Dunn K J 1980 *Phys. Rev.* B **22** 3157
[21] Yamaguchi T and Yonezawa F 1992 *J. Phys. Soc. Japan* **61** 1240
[22] Fiorentini V 1992 *Phys. Rev.* B **46** 2086